NONLINEAR $\mathcal{H}_\infty$ AND $\mathcal{W}_\infty$ CONTROL APPROACHES - A COMPARISON ANALYSIS

Daniel Neri*, Guilherme V. Raffo*†, Sergio Esteban‡

*Graduate Program in Electrical Engineering, Federal University of Minas Gerais
Belo Horizonte, MG, Brazil

†Department of Electronic Engineering, Federal University of Minas Gerais
Belo Horizonte, MG, Brasil

‡Department of Aerospace Engineering, Universidad de Sevilla
Seville, Spain.

Emails: `danielneri@ufmg.br, raffo@ufmg.br, sesteban@us.es`

Abstract— An usual approach to deal with system imperfections on the control design is the $\mathcal{H}_\infty$ control theory. The $\mathcal{H}_\infty$ theory has already been applied for controlling several systems, and their efficiency was verified in many practical experiments. Despite many advantages, the classic nonlinear $\mathcal{H}_\infty$ approach presents limitations in order to control the closed-loop transient behavior. Therefore, a new formulation of this controller in the Sobolev space was presented. In this new approach the cost variable and its time derivative are considered into the cost functional. In order to verify the advantages and disadvantages of both formulations, this paper develops nonlinear $\mathcal{H}_\infty$ controllers in the Lebesgue and Sobolev spaces for a two-wheeled self-balanced vehicle, and performs comparisons over the results.

Keywords— Mechanical systems, Robust control, nonlinear $\mathcal{H}_\infty$ control, Galerkin Approximation, Sobolev space.

Resumo— Uma abordagem usual para lidar com imperfeições do sistema no projeto de controle é a teoria de controle $\mathcal{H}_\infty$. Controladores $\mathcal{H}_\infty$ já foram aplicados em vários sistemas, e sua eficiência verificada por vários experimentos. Apesar das vantagens, a abordagem não linear clássica apresenta limitações no sentido de controlar o comportamento transiente do sistema em malha fechada. Portanto, uma nova formulação desses controladores no espaço de Sobolev foi apresentada para lidar com esses problemas. Nessa nova formulação a variável de custo e a sua derivada temporal são consideradas dentro do funcional de custo. Portanto, este artigo desenvolve controladores $\mathcal{H}_\infty$ não linear nos espaços de Lebesgue e Sobolev para um veículo de duas rodas baseado em pendulo invertido. Adicionalmente, os resultados são comparados para verificar as vantagens e desvantagens de cada controlador.

Palavras-chave— Sistemas mecânicos, Controle robusto, Controle $\mathcal{H}_\infty$ não linear, Aproximação de Galerkin, Espaço Sobolev.

1 INTRODUCTION

An usual approach to deal with system imperfections on the control design is the $\mathcal{H}_\infty$ theory (Başar and Bernhard, 2008; Van Der Schaft and Van Der Schaft, 2000). Although it has been originally formulated on the frequency domain, in Doyle et al. (1989) it was reformulated in the Lebesgue space to deal with systems represented in the state-space, which received considerable attention in the past decades. $\mathcal{H}_\infty$ controllers have already been applied for controlling several systems, and their efficiency was verified in many practical experiments. Despite many advantages, this classic formulation presents deficiencies in order to control the closed-loop transient behavior. Therefore, to overcome this issue, in Aliyu and Boukas (2011) a new formulation of this controller, in the Sobolev space, is presented. In this new approach, the cost variable and its time derivatives are considered into the cost functional. It is expected that the resulting controller presents improved transient and steady-state behavior.[1]

As the classic approach, the nonlinear $\mathcal{W}_\infty$ controller can also be formulated via dynamic-programing, from which the optimization problem results in solving the nonlinear first-order partial differential equation (PDE) called the Hamilton-Jacobi-Bellman-Isaacs (HJBI) equation. For linear systems, the HJBI equation results in a Riccati matrix equation, in which efficient computational methods can be used to compute the solution. However, for nonlinear systems the resulting HJBI equation is hard to solve analytically. In particular, according to Aliyu and Boukas (2011), the resulting HJBI PDE from the $\mathcal{W}_\infty$ control problem is considered to be "horrendous and impossible to compute the solution".

Since the HJBI equation is difficult to solve analytically, it is interesting to approximate its solution using a numerical method. This research subject is divided into four different categories: the method of characteristics (Wise and Sedwick, 1996); series approximation (Huang and

[1] Through the text we use $\mathcal{H}_\infty$ and $\mathcal{W}_\infty$ to refer to the approaches formulated in the Lebesgue and Sobolev spaces, respectively.

Lin, 1995); regularization (Freeman and Kokotovic, 1995); finite difference element approximation (Fleming and Soner, 2006); and the Successive Galerkin Approximation Algorithms (SGAA) (Beard, 1998). In order to select the numerical procedure to be used, the main features to be considered are: 1) have guaranteed stability for finite truncations of the approximation; 2) result in a simple closed-loop control to be implemented; 3) guarantee that the approximation error goes to zero as the order of the approximation increases; 4) have a well-defined region of the state-space where the approximation is guaranteed to work; 5) have low run-time computation and memory requirements; 6) effectively deal with the curse of dimensionality; 7) give explicit bounds on the approximation error. Taking into account these issues, the SGAA is the one that provides the most interesting features.

The SGAA has been proposed in Beard (1995), with the purpose to solve the Hamilton-Jacobi-Bellman (HJB) equation. In Beard (1998), it was extended to solve the HJBI equation that arises from the classic formulation of the nonlinear $\mathcal{H}_\infty$ controller. In Cardoso and Raffo (2018), it was extended to approximate the solutions of the HJBI PDE that arises from new formulation of the $\mathcal{H}_\infty$ controller in the Sobolev space. The SGAA deals with fully and underactuated systems, being a suitable way to solve the problem.

In this work the nonlinear $\mathcal{H}_\infty$ and the $\mathcal{W}_\infty$ controllers are designed in order to control a two-wheeled self-balanced vehicle. Numerical experiments are conducted to highlight the advantages and disadvantages of each control approach.

Vehicles based on inverted pendulum can be found in many different variations as: the Furuta pendulum (Acosta et al., 2001), Pendulum on a cart (Gordillo and Aracil, 2008), the pendulum on a two-wheeled vehicle (Madero et al., 2010). They have been made popular by the vehicle called Segway©[2], which is a practical way of locomotion. From the control engineering point of view, design controllers for this type of vehicles remains a challenge. It is an underactuated and coupled mechanical system. In general these vehicles are usually affected by external disturbances, unmodeled dynamics, parameter estimation errors and noise added to the measurement reported by sensors. As a benchmark system, in the literature it is easy to find works that propose linear and nonlinear controllers for this class of vehicles, as for example LQR (Wang et al., 2010), PID (Wang, 2011), Forwarding (Madero et al., 2010), and nonlinear $\mathcal{H}_\infty$ (Raffo et al., 2015).

The following sections are structured as: Section 2 presents the nonlinear $\mathcal{H}_\infty$ and $\mathcal{W}_\infty$ control approaches; Section 3 presents the Successive Galerkin Approximation Algorithms; Section 4 presents the Galerkin approximation and how it is applied with the SGAA to approximate the solutions of the $\mathcal{H}_\infty$ and $\mathcal{W}_\infty$ control problems; In Section 5 both controllers are designed for a two-wheeled self-balanced vehicle, from which numerical experiments are conducted and the controllers' performances are evaluated; Section 6 concludes the work.

[2]http://www.segway.com/

2 Nonlinear $\mathcal{H}_\infty$ control approaches

In this section the nonlinear $\mathcal{H}_\infty$ control approach is formulated in the Lebesgue and Sobolev spaces. Consider the class of systems represented by

$$\dot{\boldsymbol{x}} = \boldsymbol{f}(\boldsymbol{x}) + \boldsymbol{g}(\boldsymbol{x})\boldsymbol{u} + \boldsymbol{k}(\boldsymbol{x})\boldsymbol{w}, \tag{1}$$

in which $\boldsymbol{x}(t) \in \mathbb{R}^n$ is the state vector, $\boldsymbol{u}(t) \in \mathbb{R}^m$ is the input vector, and $\boldsymbol{w}(t) \in \mathbb{R}^d$ is the disturbance vector. Assume that (1) is controllable and all states are measured.

2.1 Nonlinear $\mathcal{H}_\infty$ control approach formulated in the Lebesgue space

The classic nonlinear $\mathcal{H}_\infty$ control is stated in terms of the $\mathcal{L}_2$ gain of the system, in which system (1) is said to have $\mathcal{L}_2$ gain less than or equal to γ if, for all $t_f \geq 0$ and $\boldsymbol{w} \in \mathcal{L}_2(0, t_f)$, there exists a $\mathcal{H}_\infty$ index $\gamma > 0$ such that the following inequality is satisfied

$$\int_0^{t_f} ||\boldsymbol{y}(t)||^2 dt \leq \gamma^2 \int_0^{t_f} ||\boldsymbol{w}(t)||^2 dt, \tag{2}$$

where $||.||$ denotes the Euclidean norm, and

$$\boldsymbol{y}(t) = \begin{bmatrix} \boldsymbol{Q} & \boldsymbol{0} \\ \boldsymbol{0} & \boldsymbol{R} \end{bmatrix} \begin{bmatrix} \boldsymbol{x} \\ \boldsymbol{u} \end{bmatrix}$$

is the cost variable, being $\boldsymbol{Q}$ and $\boldsymbol{R}$ symmetric and positive definite matrices, that must be tuned to achieve the control requirements, and $\boldsymbol{0}$ is a zero matrix with appropriate dimension. The aim of this control problem is to achieve a bounded ratio between the energy of the cost variable and the energy of external disturbance signals.

It can be shown that the performance index associated with (2) is (Bernhard, 1995)

$$\mathcal{J}_{\mathcal{L}} = \frac{1}{2} \int_0^{tf} \left(||\boldsymbol{y}(t)||^2 - \gamma^2 ||\boldsymbol{w}(t)||^2 \right) dt. \tag{3}$$

Therefore, the classic nonlinear $\mathcal{H}_\infty$ control can be stated as the optimization problem

$$V_{\mathcal{L}}(\boldsymbol{x}, t) = \min_{\boldsymbol{u} \in \mathcal{U}} \max_{\boldsymbol{w} \in W} \left\{ \frac{1}{2} \int_0^{\infty} \left(||\boldsymbol{y}(t)||^2 - \gamma^2 ||\boldsymbol{w}(t)||^2 \right) dt \right\}, \tag{4}$$

where $\mathcal{U}$ and W are the domains where the control inputs and disturbances are defined.

In order to obtain the solution of (4), it can be formulated via dynamic programing (Kirk, 2012), from which the associated Hamiltonian is given by[3]

$$\mathcal{H}_{\mathcal{L}}\left(\frac{\partial V_{\mathcal{L}}}{\partial \boldsymbol{x}},\boldsymbol{x},\boldsymbol{u},\boldsymbol{w}\right)=\frac{\partial V_{\mathcal{L}}'}{\partial \boldsymbol{x}}\dot{\boldsymbol{x}}+\frac{1}{2}||\boldsymbol{y}(t)||^2-\frac{1}{2}\gamma^2||\boldsymbol{w}(t)||^2,$$

which in its expanded form leads to

$$\mathcal{H}_{\mathcal{L}}\left(\frac{\partial V_{\mathcal{L}}}{\partial \boldsymbol{x}},\boldsymbol{x},\boldsymbol{u},\boldsymbol{w}\right)=\frac{\partial V_{\mathcal{L}}'}{\partial \boldsymbol{x}}\Big(\boldsymbol{f}(\boldsymbol{x})+\boldsymbol{g}(\boldsymbol{x})\boldsymbol{u}+\boldsymbol{k}(\boldsymbol{x})\boldsymbol{w}\Big)$$
$$+\frac{1}{2}\boldsymbol{x}'\mathcal{Q}\boldsymbol{x}+\frac{1}{2}\boldsymbol{u}'\mathcal{R}\boldsymbol{u}-\frac{1}{2}\gamma^2\boldsymbol{w}'\boldsymbol{w}, \tag{5}$$

where $\mathcal{Q}\triangleq\boldsymbol{Q}'\boldsymbol{Q}$ and $\mathcal{R}\triangleq\boldsymbol{R}'\boldsymbol{R}$.

The optimization problem (4) consists in computing the optimal control action, $\boldsymbol{u}^*$, that minimizes the performance index (3) for the worst case of all possible disturbances, $\boldsymbol{w}^*$, affecting the system. Therefore, it can be computed by maximizing and minimizing (5) with respect to these variables, respectively, leading to[4]

$$\frac{\partial\mathcal{H}_{\mathcal{L}}}{\partial \boldsymbol{u}}=\boldsymbol{g}'\frac{\partial V_{\mathcal{L}}}{\partial \boldsymbol{x}}+\mathcal{R}\boldsymbol{u}^*=0$$
$$\boldsymbol{u}^*=-\mathcal{R}^{-1}\boldsymbol{g}'\frac{\partial V_{\mathcal{L}}}{\partial \boldsymbol{x}}, \tag{6}$$
$$\frac{\partial\mathcal{H}_{\mathcal{L}}}{\partial \boldsymbol{w}}=\boldsymbol{k}'\frac{\partial V_{\mathcal{L}}}{\partial \boldsymbol{x}}-\gamma^2\boldsymbol{w}^*=0$$
$$\boldsymbol{w}^*=\frac{1}{\gamma^2}\boldsymbol{k}'\frac{\partial V_{\mathcal{L}}}{\partial \boldsymbol{x}}. \tag{7}$$

Furthermore, ($\boldsymbol{u}^*$,$\boldsymbol{w}^*$) is the saddle point solution of the problem if the following holds

$$\mathcal{H}_{\mathcal{L}}\Big(\frac{\partial \boldsymbol{V}_{\mathcal{L}}}{\partial \boldsymbol{x}},\boldsymbol{u}^*,\boldsymbol{w}\Big)\leq\mathcal{H}_{\mathcal{L}}\Big(\frac{\partial \boldsymbol{V}_{\mathcal{L}}}{\partial \boldsymbol{x}},\boldsymbol{u}^*,\boldsymbol{w}^*\Big)\leq\mathcal{H}_{\mathcal{L}}\Big(\frac{\partial \boldsymbol{V}_{\mathcal{L}}}{\partial \boldsymbol{x}},\boldsymbol{u},\boldsymbol{w}^*\Big),$$

which can be verified by computing the second order partial derivatives of (5) as

$$\frac{\partial^2\mathcal{H}_{\mathcal{L}}}{\partial \boldsymbol{u}^2}=\mathcal{R}>0,\qquad\frac{\partial^2\mathcal{H}_{\mathcal{L}}}{\partial \boldsymbol{w}^2}=-\gamma^2\boldsymbol{I}<0,$$

where clearly $\boldsymbol{u^*}$ and $\boldsymbol{w^*}$ are the respective min and max values of the optimization problem, being $\boldsymbol{I}$ an identity matrix with appropriated dimension.

The HJBI equation associated to the problem is obtained by replacing the optimal control law (6) and the worst case of disturbances (7) in (5), which is written in a compact form, as

$$\mathcal{H}_{\mathcal{L}}\left(\frac{\partial V_{\mathcal{L}}}{\partial \boldsymbol{x}},\boldsymbol{x},\boldsymbol{u}^*,\boldsymbol{w}^*\right)=0 \tag{8}$$

with boundary condition $V_{\mathcal{L}}(\boldsymbol{0})=0$. Therefore, the classic nonlinear $\mathcal{H}_\infty$ control problem results in solving the PDE (8) in order to obtain the solution $V_{\mathcal{L}}(\boldsymbol{x})$.

2.2 Nonlinear $\mathcal{H}_\infty$ control approach formulated in the Sobolev space

Considering again system (1), the nonlinear H_∞ controller, formulated in the weighted Sobolev space, is designed in order to achieve the control law $\boldsymbol{u}\in\mathcal{U}$, for the worst case of the disturbances $\boldsymbol{w}\in W$, that minimizes the cost functional[5].

$$\mathcal{J}_{\mathcal{W}}=\frac{1}{2}||\boldsymbol{z}(t)||^2_{\mathcal{W}_{1,2,\boldsymbol{\Sigma}}}-\frac{1}{2}\gamma^2||\boldsymbol{w}(t)||^2_{\mathcal{L}_2}.$$

in which $\boldsymbol{z}(t)=\boldsymbol{x}(t)$ is the cost variable, and $\boldsymbol{\Sigma}=(\mathcal{Q},\mathcal{S})$. Therefore, the optimization problem is stated as

$$V_{\mathcal{W}}=\min_{\boldsymbol{u}\in\mathcal{U}}\max_{\boldsymbol{w}\in W}\int_0^\infty\frac{1}{2}\left(||\boldsymbol{z}(t)||^2_{\mathcal{Q}}+||\dot{\boldsymbol{z}}(t)||^2_{\mathcal{S}}-\gamma^2||\boldsymbol{w}(t)||^2\right)dt.$$

Note that, different from the classic formulation in the Lebesgue $\mathcal{L}_2$ space, in the new approach the transient and steady-state performance are reached by the presence of the time derivative of the cost variable, $\boldsymbol{z}(t)$, in the cost functional, being this latter variable independent of control inputs. Moreover, this new approach allows to tune component-wise the influence of the states and their time derivatives in the cost functional.

The control design is derived by solving a Min-Max optimization problem, which can be formulated via dynamic programming. The associated Hamiltonian is given by

$$\mathcal{H}_{\mathcal{W}}=\Big(\frac{\partial V_{\mathcal{W}}'}{\partial \boldsymbol{x}}\Big)\dot{\boldsymbol{x}}+\frac{1}{2}||\boldsymbol{z}||^2_{\mathcal{Q}}+\frac{1}{2}||\dot{\boldsymbol{z}}||^2_{\mathcal{S}}-\frac{1}{2}\gamma^2||\boldsymbol{w}||^2, \tag{9}$$

which is given in its expanded shape by

$$\begin{aligned}\mathcal{H}_{\mathcal{W}}&=\left(\frac{\partial V_{\mathcal{W}}}{\partial \boldsymbol{x}}\right)'[\boldsymbol{f}(\boldsymbol{x})+\boldsymbol{g}(\boldsymbol{x})\boldsymbol{u}+\boldsymbol{k}(\boldsymbol{x})\boldsymbol{w}] \qquad (10)\\&+\frac{1}{2}\boldsymbol{x}'\mathcal{Q}\boldsymbol{x}+\frac{1}{2}\dot{\boldsymbol{x}}\mathcal{S}\dot{\boldsymbol{x}}-\frac{1}{2}\gamma^2\boldsymbol{w}'\boldsymbol{w}\\&=\left(\frac{\partial V_{\mathcal{W}}}{\partial \boldsymbol{x}}\right)'[\boldsymbol{f}(\boldsymbol{x})+\boldsymbol{g}(\boldsymbol{x})\boldsymbol{u}+\boldsymbol{k}(\boldsymbol{x})\boldsymbol{w}]\\&+\frac{1}{2}\boldsymbol{x}'\mathcal{Q}\boldsymbol{x}+\frac{1}{2}f'\mathcal{S}f+\frac{1}{2}f'\mathcal{S}g\boldsymbol{u}+\frac{1}{2}f'\mathcal{S}k\boldsymbol{w}\\&+\frac{1}{2}\boldsymbol{u}'g'\mathcal{S}f+\frac{1}{2}\boldsymbol{u}'g'\mathcal{S}g\boldsymbol{u}+\frac{1}{2}\boldsymbol{u}'g'\mathcal{S}k\boldsymbol{w}+\frac{1}{2}\boldsymbol{w}'k'\mathcal{S}f\\&+\frac{1}{2}\boldsymbol{w}'k'\mathcal{S}g\boldsymbol{u}+\frac{1}{2}\boldsymbol{w}'k'\mathcal{S}k\boldsymbol{w}-\frac{1}{2}\gamma^2\boldsymbol{w}'\boldsymbol{w}.\end{aligned}$$

In order to obtain the worst case of the disturbance, $\boldsymbol{w}^*$, and the optimal control law, $\boldsymbol{u}^*$, the partial derivatives of (10) with respect to these variables are computed

$$\frac{\partial\mathcal{H}_{\mathcal{W}}}{\partial \boldsymbol{u}}=\boldsymbol{g}'\frac{\partial V_{\mathcal{W}}}{\partial \boldsymbol{x}}+\boldsymbol{g}'\mathcal{S}\boldsymbol{f}+\boldsymbol{g}'\mathcal{S}\boldsymbol{g}\boldsymbol{u^*}+\boldsymbol{g}'\mathcal{S}\boldsymbol{k}\boldsymbol{w^*}=0, \tag{11}$$
$$\frac{\partial\mathcal{H}_{\mathcal{W}}}{\partial \boldsymbol{w}}=\boldsymbol{k}'\frac{\partial V_{\mathcal{W}}}{\partial \boldsymbol{x}}+\boldsymbol{k}'\mathcal{S}\boldsymbol{f}+\boldsymbol{k}'\mathcal{S}\boldsymbol{g}\boldsymbol{u^*}+\boldsymbol{k}'\mathcal{S}\boldsymbol{k}\boldsymbol{w^*}-\gamma^2\boldsymbol{w^*}=0. \tag{12}$$

Therefore, by manipulating (11) and (12) leads to

$$\boldsymbol{w}^*=\left(\gamma^2\boldsymbol{I}-\boldsymbol{k}'\mathcal{S}\boldsymbol{k}+\boldsymbol{k}'\mathcal{S}\boldsymbol{g}\boldsymbol{\beta}^{-1}\boldsymbol{g}'\mathcal{S}\boldsymbol{k}\right)^{-1}\times\left[\boldsymbol{k}'\frac{\partial V_{\mathcal{W}}}{\partial \boldsymbol{x}}+\boldsymbol{k}'\mathcal{S}\boldsymbol{f}-\boldsymbol{k}'\mathcal{S}\boldsymbol{g}\boldsymbol{\beta}^{-1}\left(\boldsymbol{g}'\frac{\partial V_{\mathcal{W}}}{\partial \boldsymbol{x}}+\boldsymbol{g}'\mathcal{S}\boldsymbol{f}\right)\right], \tag{13}$$

$$\boldsymbol{u}^*=-\boldsymbol{\beta}^{-1}\left(\boldsymbol{g}'\frac{\partial V_{\mathcal{W}}}{\partial \boldsymbol{x}}+\boldsymbol{g}'\mathcal{S}\boldsymbol{f}+\boldsymbol{g}'\mathcal{S}\boldsymbol{k}\boldsymbol{w}^*\right), \tag{14}$$

---

[3] For the sake of simplicity, throughout the text some function dependencies are omitted.

[4] Throughout the text the superscript * will be used to denote the optimal value.

[5] The Weighted Sobolev $\mathcal{W}_{m,p,\boldsymbol{\Sigma}}$ − norm of a signal is defined as $||\boldsymbol{z}(t)||_{\mathcal{W}_{m,p,\boldsymbol{\Sigma}}}=\big(\sum_{\alpha=0}^{m}||\frac{d^m\boldsymbol{z}}{dt^m}||^p_{\mathcal{L}_p,\boldsymbol{\Sigma}_\alpha}\big)^{1/p}$ such that $\boldsymbol{\Sigma}=(\boldsymbol{\Sigma}_0,\boldsymbol{\Sigma}_1,...,\boldsymbol{\Sigma}_m)$ with $\boldsymbol{\Sigma}_\alpha'=\boldsymbol{\Sigma}_\alpha$ and $\boldsymbol{\Sigma}_\alpha>0$.

with $\boldsymbol{\beta} \triangleq \boldsymbol{g}'\mathcal{S}\boldsymbol{g}$, being $(\boldsymbol{u}^*, \boldsymbol{w}^*)$ the saddle-point solution of the problem, which can be verified by computing the second order partial derivatives of (10) as

$$\frac{\partial^2 \mathcal{H}_{\mathcal{W}}}{\partial \boldsymbol{u}^2} = \boldsymbol{g}'\mathcal{S}\boldsymbol{g} > 0,$$
$$\frac{\partial \mathcal{H}_{\mathcal{W}}^2}{\partial \boldsymbol{w}^2} = \boldsymbol{k}'\mathcal{S}\boldsymbol{k} - \gamma^2 \boldsymbol{I} < 0,$$

where clearly, for an appropriated selection of γ, they are the min-max extrema of the optimization problem.

In order to obtain the HJBI equation associated to this problem, it is necessary to replace (13) and (14) in (10), leading to a complex partial differential equation, which is hard to solve analytically. In Aliyu and Boukas (2011) the resulting HJBI PDE is presented, which is assumed to be intractable. Therefore, in this work an approximate solution to the HJBI is obtained through the Sucessive Galerkin Approximation Algorithm.

3 Successive Galerkin Approximation Algorithm

The HJBI equation resulting from the formulation of the nonlinear $\mathcal{H}_\infty$ control problems, in the Lebesgue and Sobolev spaces, are in a quadratic form, which is not suitable to apply directly the Galerkin's method. It presents two solutions, in which one corresponds to the desired stabilizing control law. Therefore, to solve this problem the SGAA is applied. This algorithm decreases the problem's complexity to a non-quadratic form leading to a single solution.

The algorithms used to solve the nonlinear $\mathcal{H}_\infty$ control problems in the Lebesgue and Sobolev spaces are presented in Algorithms 1 and 2, respectively. Although the number of iterations in these algorithms goes from 1 to ∞, the stopping criterions $V^{(i,j)} = V^{(i,j+1)}$ and $V^{(i,\infty)} = V^{(i+1,\infty)}$ are used when seeking the optimal solution of the HJBI equation.

In particular, $\boldsymbol{u}^{(i)}$ will ensure stability of the system (1) on the same region of the state space as $\boldsymbol{u}^{(0)}$ does. In addition, as stated in (Beard et al., 1998), considering the algorithms 1 and 2, it is not possible to find an admissible control that can stabilize an initial condition that is unstable. The convergence proof of the algorithms 1 and 2, follows the same procedure as in (Beard, 1998). Furthermore, the $\mathcal{H}_\infty$ index γ must be selected such that the problem is feasible, if it is not true the algorithm does not converge.

In order to use the proposed algorithms and approximate the solutions $V_{\mathcal{L}}(\boldsymbol{x})$ and $V_{\mathcal{W}}(\boldsymbol{x})$ of Hamiltonians $\mathcal{H}_{\mathcal{L}}$ and $\mathcal{H}_{\mathcal{W}}$, the Galerkin's method is applied. In the next section, the general formulation of the Galerkin's method is briefly described, followed by its design to approximate a

Algorithm 1 SGAA to nonlinear $\mathcal{H}_\infty$ control approach in the Lebesgue space.

Let $\boldsymbol{u}^{(0)}$ be any initial stabilizing control law for the system (1) with $\boldsymbol{w} = \boldsymbol{0}$ and stability region Ω.
Set $\boldsymbol{w}^{(0,0)} = \boldsymbol{0}$
for $i = 0$ to ∞ **do**
  for $j = 0$ to ∞ **do**
    Solve for $V_{\mathcal{L}}^{(i,j)}$ from:

$$\left(\frac{\partial V_{\mathcal{L}}^{(i,j)}}{\partial \boldsymbol{x}}\right)' \left[\boldsymbol{f}(\boldsymbol{x}) + \boldsymbol{g}(\boldsymbol{x})\boldsymbol{u}^{(i)} + \boldsymbol{k}(\boldsymbol{x})\boldsymbol{w}^{(i,j)}\right] + \frac{1}{2}\boldsymbol{x}'\mathcal{Q}\boldsymbol{x} + \frac{1}{2}\boldsymbol{u}'^{(i)}\mathcal{R}\boldsymbol{u}^{(i)} - \frac{1}{2}\gamma^2 \boldsymbol{w}'^{(i,j)}\boldsymbol{w}^{(i,j)} = 0$$

    Update the Disturbance:

$$\boldsymbol{w}^{(i,j+1)} = \frac{1}{\gamma^2}\boldsymbol{k}'\frac{\partial V_{\mathcal{L}}^{(i,j)}}{\partial \boldsymbol{x}}$$

  end for
  Update the Control:

$$\boldsymbol{u}^{(i+1)} = -\mathcal{R}^{-1}\boldsymbol{g}'\frac{\partial V_{\mathcal{L}}^{(i,\infty)}}{\partial \boldsymbol{x}}$$

end for

Algorithm 2 SGAA to nonlinear $\mathcal{H}_\infty$ control approach in the Sobolev space.

Let $\boldsymbol{u}^{(0)}$ be any initial stabilizing control law for the system (1) with $\boldsymbol{w} = \boldsymbol{0}$ and stability region Ω.
Set $\boldsymbol{w}^{(0,0)} = \boldsymbol{0}$
for $i = 0$ to ∞ **do**
  for $j = 0$ to ∞ **do**
    Solve for $V^{(i,j)}$ from:

$$\left(\frac{\partial V_{\mathcal{W}}^{(i,j)}}{\partial \boldsymbol{x}}\right)' \left[\boldsymbol{f}(\boldsymbol{x}) + \boldsymbol{g}(\boldsymbol{x})\boldsymbol{u}^{(i)} + \boldsymbol{k}(\boldsymbol{x})\boldsymbol{w}^{(i,j)}\right] + \frac{1}{2}\left(||\boldsymbol{z}||^2 + ||\dot{\boldsymbol{z}}||^2 - \gamma^2 ||\boldsymbol{w}^{(i,j)}||^2\right) = 0$$

    Update the Disturbance:

$$\boldsymbol{w}^{(i,j+1)} = \left(\gamma^2 \boldsymbol{I} - \boldsymbol{k}'\mathcal{S}\boldsymbol{k} + \boldsymbol{k}'\mathcal{S}\boldsymbol{g}\boldsymbol{\beta}^{-1}\boldsymbol{g}'\mathcal{S}\boldsymbol{k}\right)^{-1} \left[\boldsymbol{k}'\frac{\partial V_{\mathcal{W}}^{(i,j)}}{\partial \boldsymbol{x}} + \boldsymbol{k}'\mathcal{S}\boldsymbol{f} - \boldsymbol{k}'\mathcal{S}\boldsymbol{g}\boldsymbol{\beta}^{-1}\left(\boldsymbol{g}'\frac{\partial V_{\mathcal{W}}^{(i,j)}}{\partial \boldsymbol{x}} + \boldsymbol{g}'\mathcal{S}\boldsymbol{f}\right)\right]$$

  end for
  Update the Control:

$$\boldsymbol{u}^{(i+1)} = -\boldsymbol{\beta}^{-1}\left(\boldsymbol{g}'\frac{\partial V_{\mathcal{W}}^{(i,\infty)}}{\partial \boldsymbol{x}} + \boldsymbol{g}'\mathcal{S}\boldsymbol{f} + \boldsymbol{g}'\mathcal{S}\boldsymbol{k}\boldsymbol{w}^{(i,\infty)}\right)$$

end for

solution of the HJBI equations presented in Section 2.

4 Galerkin approximation

Galerkin's method is commonly used to solve partial differential equations (Mikhlin and Smolitskiy, 1967). In this work, it is applied to achieve the solutions $V_{\mathcal{L}}(\boldsymbol{x})$ and $V_{\mathcal{W}}(\boldsymbol{x})$ of Hamiltonians $\mathcal{H}_{\mathcal{L}}$ and $\mathcal{H}_{\mathcal{W}}$, respectively. Therefore, by rewriting these PDEs in a generic compact form

$$\mathcal{A}(V(\boldsymbol{x})) = \boldsymbol{0}, \tag{15}$$

the first step for applying the Galerkin's method is to place the solution of (15) in the Hilbert space, $V(\boldsymbol{x}) \in \mathcal{L}_2(\Omega)$. It is obtained by constraining this solution to a compact subset of the space Ω. The Galerkin approach assumes that a set of functions $\Phi(\boldsymbol{x}) = [\phi_1(\boldsymbol{x})\ \phi_2(\boldsymbol{x})\ ...\ \phi_\infty(\boldsymbol{x})]$ can be selected, satisfying the problem's boundary condition, with $\Phi(\boldsymbol{x})$ being a complete basis of the space Ω. This implies that there exist coefficients c_j such that

$$\big|\big|V(\boldsymbol{x}) - \sum_{j=1}^{\infty} c_j \phi_j(\boldsymbol{x})\big|\big|_{\mathcal{L}_2(\Omega)} = 0.$$

Nevertheless, in practice the set of basis function is truncated with a finite number of terms

$$V_N(\boldsymbol{x}) = \sum_{j=1}^{N} c_j \phi_j(\boldsymbol{x}) = \boldsymbol{c}^T \Phi(\boldsymbol{x}), \tag{16}$$

which may not be a complete basis in the domain of interest[6]. Thus, by applying (16) in (15), it generates the following error approach,

$$\mathcal{A}(V_N(\boldsymbol{x})) = \mathrm{Error}(\boldsymbol{x}).$$

In the Galerkin's method, the vector of coefficients $\boldsymbol{c}$ are determined by setting the projection of the error on the finite basis $\Phi(\boldsymbol{x})$ equal to zero, $\forall \boldsymbol{x} \in \Omega$, as follows

$$< \mathcal{A}(V_N(\boldsymbol{x})), \boldsymbol{\phi}_j(\boldsymbol{x}) >= \int_\Omega \mathcal{A}(V_N(\boldsymbol{x}))\boldsymbol{\phi}_j(\boldsymbol{x}) d\boldsymbol{\Omega} = 0, \tag{17}$$

with $j = 1,\ 2,\ ...\ N$.

Therefore, taking into account the Algorithm 1 and the Hamiltonian (5), the procedure to achieve an approximate solution $V_{\mathcal{L}}(\boldsymbol{x})$, $\forall \boldsymbol{x} \in \Omega$, is conducted as

$$\int_\Omega \Big[\Big(\frac{\partial \boldsymbol{\Phi}'\boldsymbol{c}}{\partial \boldsymbol{x}}\Big)'\big[\boldsymbol{f}(\boldsymbol{x}) + \boldsymbol{g}(\boldsymbol{x})\boldsymbol{u} + \boldsymbol{k}(\boldsymbol{x})\boldsymbol{w}\big] + \frac{1}{2}\big(||\boldsymbol{y}||^2 - \gamma^2||\boldsymbol{w}||^2\big)\Big]\boldsymbol{\Phi}' d\Omega = 0,$$

leading to

$$\boldsymbol{c}' \int_\Omega \nabla\boldsymbol{\Phi}'\big[\boldsymbol{f}(\boldsymbol{x}) + \boldsymbol{g}(\boldsymbol{x})\boldsymbol{u} + \boldsymbol{k}(\boldsymbol{x})\boldsymbol{w}\big]\boldsymbol{\Phi}' d\Omega = -\frac{1}{2}\int_\Omega \big(||\boldsymbol{y}||^2 - \gamma^2||\boldsymbol{w}||^2\big)\boldsymbol{\Phi}' d\Omega.$$

[6]The finite set of basis functions must be selected to provide a small approximation error in the domain of interest, ensuring the algorithms' convergence.

Therefore, for this problem the vector of coefficients $\boldsymbol{c}$ is obtained by

$$\boldsymbol{c}' = \Big(-\frac{1}{2}\int_\Omega \big(||\boldsymbol{y}||^2 - \gamma^2||\boldsymbol{w}||^2\big)\boldsymbol{\Phi}' d\Omega\Big) \times \Big(\int_\Omega \nabla\boldsymbol{\Phi}'\big[\boldsymbol{f}(\boldsymbol{x}) + \boldsymbol{g}(\boldsymbol{x})\boldsymbol{u} + \boldsymbol{k}(\boldsymbol{x})\boldsymbol{w}\big]\boldsymbol{\Phi}' d\Omega\Big)^{-1}. \tag{18}$$

For the Algorithm 2 with the Hamiltonian (9), the procedure to achieve an approximate solution $V_{\mathcal{W}}(\boldsymbol{x})$, $\forall \boldsymbol{x} \in \Omega$, is conducted as

$$\int_\Omega \Big[\Big(\frac{\partial \boldsymbol{\Phi}'\boldsymbol{c}}{\partial \boldsymbol{x}}\Big)'\big[\boldsymbol{f}(\boldsymbol{x}) + \boldsymbol{g}(\boldsymbol{x})\boldsymbol{u} + \boldsymbol{k}(\boldsymbol{x})\boldsymbol{w}\big] + \frac{1}{2}\big(||\boldsymbol{z}||^2 + ||\dot{\boldsymbol{z}}||^2 - \gamma^2||\boldsymbol{w}||^2\big)\Big]\boldsymbol{\Phi}' d\Omega = 0,$$

leading to

$$\boldsymbol{c}' \int_\Omega \nabla\boldsymbol{\Phi}'\big[\boldsymbol{f}(\boldsymbol{x}) + \boldsymbol{g}(\boldsymbol{x})\boldsymbol{u} + \boldsymbol{k}(\boldsymbol{x})\boldsymbol{w}\big]\boldsymbol{\Phi}' d\Omega = -\frac{1}{2}\int_\Omega \big(||\boldsymbol{z}||^2 + ||\dot{\boldsymbol{z}}||^2 - \gamma^2||\boldsymbol{w}||^2\big)\boldsymbol{\Phi}' d\Omega,$$

For the nonlinear $\mathcal{W}_\infty$ control problem the vector of coefficients $\boldsymbol{c}$ is given by

$$\boldsymbol{c}' = \Big(-\frac{1}{2}\int_\Omega \big(||\boldsymbol{z}||^2 + ||\dot{\boldsymbol{z}}||^2 - \gamma^2||\boldsymbol{w}||^2\big)\boldsymbol{\Phi}' d\Omega\Big) \times \Big(\int_\Omega \nabla\boldsymbol{\Phi}'\big[\boldsymbol{f}(\boldsymbol{x}) + \boldsymbol{g}(\boldsymbol{x})\boldsymbol{u} + \boldsymbol{k}(\boldsymbol{x})\boldsymbol{w}\big]\boldsymbol{\Phi}' d\Omega\Big)^{-1}. \tag{19}$$

In the next section, equations (18) and (19) are computed with Algorithms 1 and 2 in order to design the nonlinear $\mathcal{H}_\infty$ and $\mathcal{W}_\infty$ controllers for a two-wheeled self-balanced vehicle.

5 Numerical Results

To corroborate the controllers' efficiency, in this section numerical experiments are conducted with a two-wheeled self-balanced vehicle, illustrated in Figure 1.

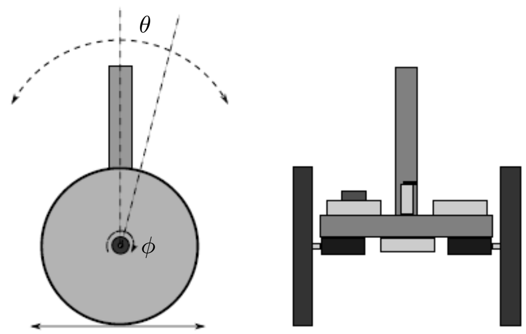

Figure 1: The two-wheeled vehicle.

The vehicle's model was obtained from Raffo et al. (2015), which is given by

$$\boldsymbol{M}(\boldsymbol{q})\ddot{\boldsymbol{q}} + \boldsymbol{C}(\boldsymbol{q}, \dot{\boldsymbol{q}})\dot{\boldsymbol{q}} + \boldsymbol{K}(\dot{\boldsymbol{q}}) + \boldsymbol{G}(\boldsymbol{q}) = \boldsymbol{F}(\boldsymbol{q})u + \boldsymbol{w}, \tag{20}$$

with

$$
\boldsymbol{M}(\boldsymbol{q}) = \begin{bmatrix} (M+m)r^2 + I_r & mlr\cos(\theta) \\ mlr\cos(\theta) & ml^2 + I_p \end{bmatrix}, \ \boldsymbol{q} = \begin{bmatrix} \phi \\ \theta \end{bmatrix},
$$

$$
\boldsymbol{C}(\boldsymbol{q}, \dot{\boldsymbol{q}}) = \begin{bmatrix} 0 & -mlr\sin(\theta)\dot{\theta} \\ 0 & 0 \end{bmatrix}, \qquad \boldsymbol{K}(\dot{\boldsymbol{q}}) = \begin{bmatrix} k\dot{\phi} \\ -k\dot{\phi} \end{bmatrix},
$$

$$
\boldsymbol{G}(\boldsymbol{q}) = \begin{bmatrix} 0 \\ -mgl\sin(\theta) \end{bmatrix}, \ \boldsymbol{F}(\boldsymbol{q}) = \begin{bmatrix} 1 \\ -1 \end{bmatrix}, \ \boldsymbol{w} = \begin{bmatrix} w_1 \\ w_2 \end{bmatrix},
$$

where $u \in \mathbb{R}$ is the torque applied on vehicles' wheels, $w_1, w_2 \in \mathcal{L}_2$ are disturbances applied to the system, m is the mass of the pendulum, M is the mass of the wheels, l is the distance from the axle to the pendulum center of mass, r is the wheel's radius, I_p is the pendulum moment of inertia, I_r is the inertia of the wheel, k is the static friction of the motor, and g is the gravity acceleration. The physical parameters used on numerical simulations are presented in Table 1.

Table 1: Vehicle parameters

Parameter	Value	Unit of Measure
I_r	0.0421	$kg \cdot m^2$
Ip	0.201	$kg \cdot m^2$
k	0.00215	$N \cdot m \cdot s/rad$
m	2.75	kg
M	3.75	kg
l	0.1435	m
r	0.25	m
g	9.8	m/s^2

The equations of motion (20) are represented in the state-space standard form (1), leading to

$$
\boldsymbol{f}(\boldsymbol{x}) = \begin{bmatrix} \dot{\theta} \\ -\boldsymbol{M}^{-1}(\boldsymbol{q})\left[\boldsymbol{C}(\boldsymbol{q}, \dot{\boldsymbol{q}})\dot{\boldsymbol{q}} + \boldsymbol{K}(\dot{\boldsymbol{q}}) + \boldsymbol{G}(\boldsymbol{q})\right] \end{bmatrix},
$$

$$
\boldsymbol{g}(\boldsymbol{x}) = \begin{bmatrix} 0 \\ \boldsymbol{M}^{-1}(\boldsymbol{q})\boldsymbol{F}(\boldsymbol{q}) \end{bmatrix}, \qquad \boldsymbol{k}(\boldsymbol{x}) = \begin{bmatrix} 0 & 0 \\ \boldsymbol{M}^{-1}(\boldsymbol{q}) \end{bmatrix},
$$

with $\boldsymbol{x} = \begin{bmatrix} \theta & \dot{\phi} & \dot{\theta} \end{bmatrix}'$.

With the objective of regulating the states around their equilibrium point $\boldsymbol{x} = \boldsymbol{0}$, the nonlinear $\mathcal{H}_\infty$ and $\mathcal{W}_\infty$ controllers are designed by iterating Algorithms 1 and 2 and considering the Galerkin's approximations (18) and (19). A complete polynomial basis with degree four is used as basis functions, which is given by

$$
\Phi(\boldsymbol{x}) = \begin{bmatrix} \theta & \dot{\phi} & \dot{\theta} & \dot{\phi}\theta & \theta\dot{\theta} & \dot{\phi}\dot{\theta} & \dot{\phi}^2 & \theta^2 & \dot{\theta}^2 & \cdots & \theta^4 & \dot{\phi}^4 & \dot{\theta}^4 \end{bmatrix}.
$$

The set Ω is the domain of interest in which the controller ensures stability to the system, and it must be selected as the region of the state-space in which the system works in. In this paper it is selected as $\Omega = \theta_\Omega \times \dot{\phi}_\Omega \times \dot{\theta}_\Omega = [-\frac{\pi}{4}, \frac{\pi}{4}] \times [-3, 3] \times [-1.2, 1.2]$.

The integrals presented in (18) and (19) are computed using Gaussian quadrature with one point

$$
\int_a^b \psi(\xi)d\xi = (b-a)\psi(\frac{b+a}{2}).
$$

In order to apply the Gaussian quadrature, the domain Ω is split in several squares with dimension $\Delta = 0.1$. The integrated functions are assumed uncoupled, such that the following holds

$$
\int_a^b \int_c^d \int_e^f \psi(\theta, \dot{\phi}, \dot{\theta}) d\theta \ d\dot{\phi} \ d\dot{\theta} = \int_a^b \psi(\theta)d\theta \int_c^d \psi(\dot{\phi})d\dot{\phi} \int_e^f \psi(\dot{\theta})d\dot{\theta}.
$$

During the iterations of Algorithms 1 and 2, the coefficients $\boldsymbol{c}$ of the Galerkin's Method converge asymptotically to the solution. Therefore, in order to decrease the computational time taken to obtain the solution, it is used the stopping criteria $||\boldsymbol{c}^{i-1} - \boldsymbol{c}^i|| < 0.1$. In addition, a linear state feedback LQR controller was designed as the initial stabilizing control law for both controllers, which resulted in

$$
u^{(0)} = \begin{bmatrix} 11.3132 & 1.0022 & 3.2589 \end{bmatrix} \boldsymbol{x}.
$$

In order to perform a fair comparison of the results, the $\mathcal{H}_\infty$ attenuation level was set as $\gamma = 5$. Additionally, the controllers were tunned to provide almost the same settling time, using the criteria of 5%, as shown in Figure 2. This choice resulted in the following adjustments $\mathcal{Q} = \boldsymbol{I}$, $\mathcal{R} = 1$, and $\mathcal{S} = \mathrm{diag}([0.64 \ \ 0.01 \ \ 0.01])$.

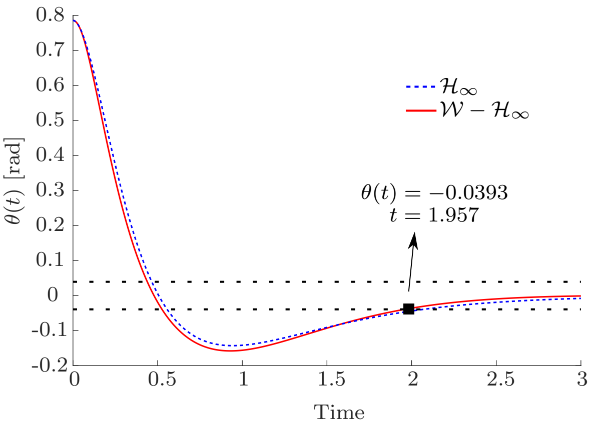

Figure 2: Settling time starting from initial condition $\boldsymbol{x} = [\frac{\pi}{4} \ 0 \ 0]'$.

By executing the SGAA, the following solutions were obtained for the HJBI equations,

$$
\begin{aligned}
V_{\mathcal{L}}(\boldsymbol{x}) = & \frac{\dot{\phi}^4}{500} + \frac{\dot{\phi}^3\theta}{125} + \frac{\dot{\phi}^3\dot{\theta}}{200} - \frac{147\dot{\phi}^2\theta^2}{1000} + \frac{23\dot{\phi}^2\theta\dot{\theta}}{1000} \\
& - \frac{\dot{\phi}^2\theta}{1000} + \frac{3\dot{\phi}^2\dot{\theta}^2}{500} + \frac{579\dot{\phi}^2}{1000} - \frac{689\dot{\phi}\theta^3}{1000} - \frac{9\dot{\phi}\theta^2\dot{\theta}}{40} \\
& - \frac{\dot{\phi}\theta^2}{250} + \frac{13\dot{\phi}\theta\dot{\theta}^2}{1000} - \frac{\dot{\phi}\theta\dot{\theta}}{1000} + \frac{3487\dot{\phi}\theta}{1000} + \frac{3\dot{\phi}\dot{\theta}^3}{1000} \\
& + \frac{991\dot{\phi}\dot{\theta}}{1000} + \frac{\dot{\phi}}{500} + \frac{\theta^4}{200} - \frac{43\theta^3\dot{\theta}}{100} + \frac{3\theta^3}{1000} \\
& - \frac{31\theta^2\dot{\theta}^2}{500} - \frac{\theta^2\dot{\theta}}{1000} + \frac{4783\theta^2}{500} + \frac{3\theta\dot{\theta}^3}{1000} + \frac{569\theta\dot{\theta}}{125} \\
& + \frac{31\theta}{1000} + \frac{641\dot{\theta}^2}{1000} + \frac{\dot{\theta}}{1000},
\end{aligned}
$$

$$
\begin{aligned}
V_{\mathcal{W}}(\boldsymbol{x}) = {} & \frac{\dot\phi^4}{1000} + \frac{3\dot\phi^3\theta}{1000} + \frac{3\dot\phi^3\dot\theta}{1000} - \frac{83\dot\phi^2\theta^2}{1000} + \frac{\dot\phi^2\theta\dot\theta}{100} \\
& + \frac{\dot\phi^2\dot\theta^2}{250} + \frac{231\dot\phi^2}{500} - \frac{67\dot\phi\theta^3}{125} - \frac{77\dot\phi\theta^2\dot\theta}{500} - \frac{\dot\phi\theta^2}{500} \\
& + \frac{\dot\phi\theta\dot\theta^2}{200} + \frac{69\dot\phi\theta}{25} + \frac{\dot\phi\dot\theta^3}{500} + \frac{92\dot\phi\dot\theta}{125} - \frac{\dot\phi}{1000} \\
& - \frac{419\theta^4}{500} - \frac{541\theta^3\dot\theta}{1000} - \frac{\theta^3}{200} - \frac{23\theta^2\dot\theta^2}{250} - \frac{\theta^2\dot\theta}{500} \\
& + \frac{2869\theta^2}{500} - \frac{\theta\dot\theta^3}{1000} + \frac{1313\theta\dot\theta}{500} + \frac{\theta}{1000} + \frac{399\dot\theta^2}{1000} \\
& - \frac{\dot\theta}{1000}.
\end{aligned}
$$

The system was simulated starting from the initial condition $\boldsymbol{x}(0) = [\frac{\pi}{4} \;\; 0 \;\; 0]'$. The obtained results are presented in Figure 3.

At the beginning, the pendulum starts displaced from the desired upper vertical position and asymptotically converges to it, remaining in this position until external disturbances are applied. Due to the coupled dynamics of the system, the effects of external disturbances affect all states.

Since the nonlinear $\mathcal{W}_\infty$ controller considers the time derivative of the cost variable on the cost functional, it reacts faster to external disturbances than the $\mathcal{H}_\infty$ controller, presenting smaller overshoots with faster transients.

The control input and the states signals were evaluated by means of the Integral of the Absolute Value of the Control Input's Time Derivative (IAVU) and the Integral of the Square Error (ISE) performance indexes, which are shown in Table 2. Note that, although the results do not present significant differences on states $\theta(t)$ and $\dot\theta(t)$, the $\mathcal{W}_\infty$ controller achieved considerable improvement on the wheels' velocity, with less control effort.

Table 2: Table of Performance Index.

P. Index	Computed by	$\mathcal{H}_\infty$	$\mathcal{W}_\infty$
IAVU	$\int_0^{t_f} \left\lvert \frac{d\boldsymbol{u(t)}}{dt} \right\rvert dt$	16.809	**16.117**
ISE	$\int_0^{t_f} \theta^2(t)dt$	**1.199**	1.217
	$\int_0^{t_f} \dot\phi^2(t)dt$	85.254	**49.682**
	$\int_0^{t_f} \dot\theta^2(t)dt$	**1.604**	1.736

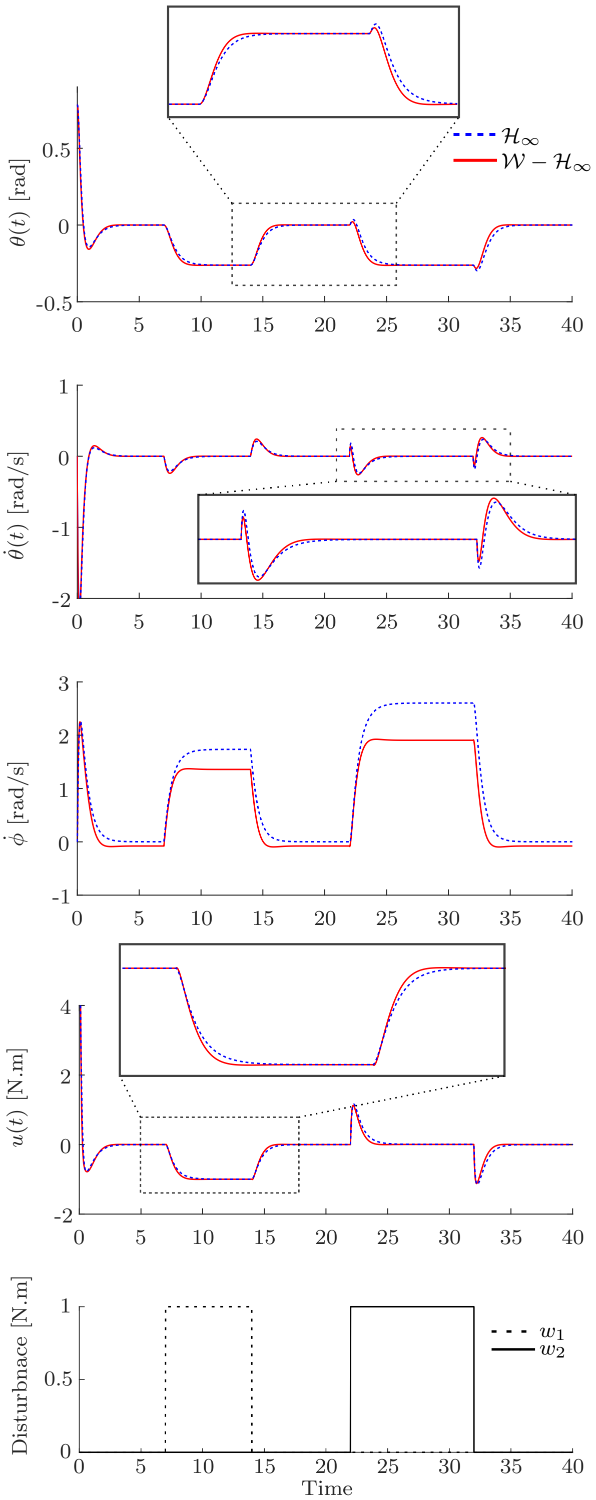

Figure 3: Vehicle states, applied control input and external disturbances.

6 CONCLUSIONS

Considering the nonlinear $\mathcal{H}_\infty$ control approaches in the Lebesgue and the Sobolev spaces, this work designed nonlinear controllers for a two-wheeled self-balanced vehicle. The HJBI equations that arise from both optimization problems were solved using the Galerkin Approximation Algorithm. Numerical experiments were conducted in order to provide a comparison analysis between both designed control laws.

The controller resulting from the $\mathcal{H}_\infty$ approach formulated in the Sobolev space presented smaller overshoot, faster reaction to external disturbances, with less control effort.

Future works include parallelize the Sucessive Galerkin Approximation Algorithm to overcome the curse of dimensionality and apply it to develop controllers for systems with higher dimension.

Acknowledgments

This work was supported by the projects INCT InSAC and Universal under the grants CNPq 465755/2014-3 and 426392/2016-7, and also by the Brazilian agencies CAPES and FAPEMIG.

References

Acosta, J., Aracil, J. and Gordillo, F. (2001). Nonlinear control strategies for the furuta pendulum, *Control and intelligent systems* **29**(3): 101–107.

Aliyu, M. and Boukas, E. K. (2011). Extending nonlinear $\mathcal{H}_2$, $\mathcal{H}_\infty$ optimisation to $\mathcal{W}_{1,2}$, $\mathcal{W}_{1,\infty}$ spaces - part i: optimal control, *International Journal of Systems Science* **42**(5): 889–906.

Başar, T. and Bernhard, P. (2008). *H-infinity optimal control and related minimax design problems: a dynamic game approach*, Springer Science & Business Media.

Beard, R. (1995). *Improving the closed-looped performance of nonlinear systems*, PhD thesis, Rensselaer Polutechnic Institute.

Beard, R. W. (1998). Successive galerkin approximation algorithms for nonlinear optimal and robust control, *International Journal of Control* **71**(5): 717–743.

Beard, R. W., Saridis, G. N. and Wen, J. T. (1998). Approximate solutions to the time-invariant hamilton–jacobi–bellman equation, *Journal of Optimization theory and Applications* **96**(3): 589–626.

Bernhard, P. (1995). *$\mathcal{H}_\infty$-optimal control and related minimax design problems: a dynamic game approach*, Birkhäuser.

Cardoso, D. N. and Raffo, G. V. (2018). Approximated solutions to the nonlinear $\mathcal{H}_2$ and $\mathcal{H}_\infty$ control approaches formulated in the sobolev space, *Proccedings of the European Control Conference 2018*.

Doyle, J. C., Glover, K., Khargonekar, P. P. and Francis, B. A. (1989). State-space solutions to standard $\mathcal{H}_2$ and $\mathcal{H}_\infty$ control problems, *IEEE Transactions on Automatic control* **34**(8): 831–847.

Fleming, W. H. and Soner, H. M. (2006). *Controlled Markov processes and viscosity solutions*, Vol. 25, Springer Science & Business Media.

Freeman, R. and Kokotovic, P. (1995). Optimal nonlinear controllers for feedback linearizable systems, *American Control Conference, Proceedings of the 1995*, Vol. 4, IEEE, pp. 2722–2726.

Gordillo, F. and Aracil, J. (2008). A new controller for the inverted pendulum on a cart, *International Journal of Robust and Nonlinear Control* **18**(17): 1607–1621.

Huang, J. and Lin, C.-F. (1995). Numerical approach to computing nonlinear h-infinity control laws, *Journal of Guidance, Control, and Dynamics* **18**(5): 989–994.

Kirk, D. E. (2012). *Optimal control theory: an introduction*, Courier Corporation.

Madero, V., Aracil, J. and Gordillo, F. (2010). A nonlinear control law for two-wheeled self-balanced vehicles, *MELECON 2010-2010 15th IEEE Mediterranean Electrotechnical Conference*, IEEE, pp. 1557–1562.

Mikhlin, S. G. and Smolitskiy, K. L. (1967). *Approximate methods for solution of differential and integral equations*, American Elsevier New York.

Raffo, G. V., Ortega, M. G., Madero, V. and Rubio, F. R. (2015). Two-wheeled self-balanced pendulum workspace improvement via underactuated robust nonlinear control, *Control Engineering Practice* **44**: 231–242.

Van Der Schaft, A. J. and Van Der Schaft, A. (2000). *L2-gain and passivity techniques in nonlinear control*, Vol. 2, Springer.

Wang, H., Dong, H., He, L., Shi, Y. and Zhang, Y. (2010). Design and simulation of lqr controller with the linear inverted pendulum, *Electrical and Control Engineering (ICECE), 2010 International Conference on*, IEEE, pp. 699–702.

Wang, J.-J. (2011). Simulation studies of inverted pendulum based on pid controllers, *Simulation Modelling Practice and Theory* **19**(1): 440–449.

Wise, K. A. and Sedwick, J. L. (1996). Nonlinear h-infinity optimal control for agile missiles, *Journal of guidance, control, and dynamics* **19**(1): 157–165.